Pea			
0			
1			
2–3			2.75
4		6	5.5
5	3	8	7.6 (?)
6	2	10	—
			—

TABLE 9.3 Some Numerical Values Pertinent to the ^{57}Fe Mössbauer Line

Transition energy	$E_\gamma = 14.4 \times 10^3$ eV
Internal conversion coefficient	$\alpha = e/\gamma = 15$
Lifetime	$t = 1.4 \times 10^{-7}$ s
Relative width	$\Delta\nu/\nu = 3 \times 10^{-13}$
Recoil energy of free nucleus	$E_R = 0.19 \times 10^{-2}$ eV
Debye temperature (Mössbauer)	$\Theta_D = 490$ K
Probability for recoilless transition at room temperature	$f = 0.80$
Cross section for resonant absorption	$\sigma_0 = 15 \times 10^{-19}$ cm^2
Natural abundance of ^{57}Fe	2.17%

A very complete description of the Mössbauer effect, including reprints of the most important papers, will be found in H. Frauenfelder's *The Mössbauer Effect* (W. A. Benjamin, New York, 1962); this reference should be fully adequate until the student finds it necessary to consult the current literature.

9.4. DETECTION OF COSMIC RAYS

9.4.1. Flux, Composition, and Detection of Cosmic Rays

The earth is continuously bombarded by a flux of high-energy particles that originate outside of the solar system. These are mainly protons but the primary cosmic ray flux also contains a fraction of light nuclei. When these particles reach the earth's atmosphere they cause nuclear interactions so that at sea level we observe only the final products of the nuclear cascade.[18]

The interaction of the primary protons with the oxygen and nitrogen nuclei of the atmosphere results in the production of secondaries including unstable particles such as $\pi^\pm$ mesons, $K^\pm$ mesons, and others. These in turn decay by the weak interaction into lighter particles, including muons, electrons, and neutrinos. Electrons and high-energy γ-rays also interact rapidly, giving rise to electromagnetic showers as discussed in Section 8.2.6. Since the earth's atmosphere is equivalent to ten nuclear interaction lengths, all strongly interacting particles are absorbed before reaching sea level.[19] What is observed (at sea level) is a "hard component" consisting of $\mu^\pm$ (muons) and a "soft component" consisting of $e^\pm$ and low-energy γ-rays.

The total flux per unit solid angle around the vertical, crossing unit horizontal area is

$$1.1 \times 10^2/\text{m}^2\text{-sr-s}, \tag{9.22a}$$

where 75% of the flux is in the hard component. The angular distribution is approximately $\cos^2\theta$ (with $\theta = 0$ at the zenith). It is also useful to know

[18] A good reference on cosmic rays in general can be found online from the Particle Data Group at http://pdg.lbl.gov in the "Reviews" section under "Astrophysics and Cosmology."

[19] Some of these unstable particles were first observed and studied at high mountain altitudes or by baloon-borne detectors. Today such subnuclear particles are produced profusely by particle accelerators, but cosmic rays are still used for the study of the very highest energies.

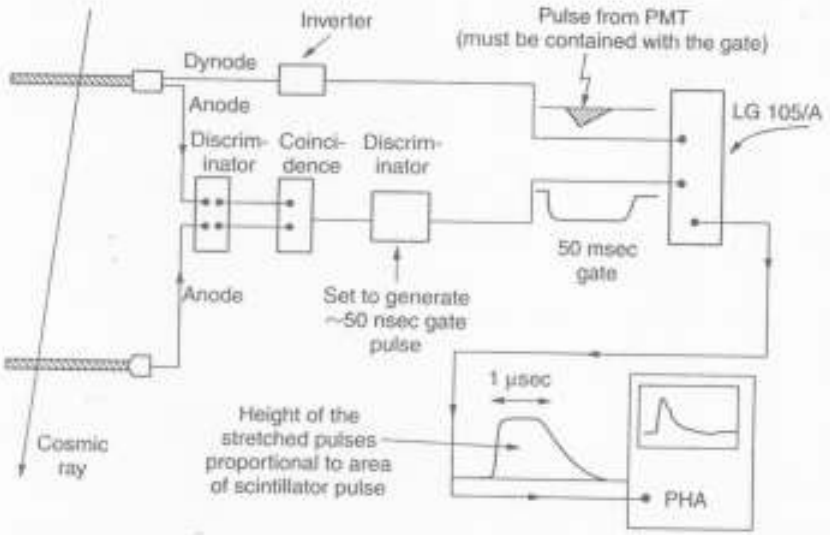

IGURE 9.20 Typical layout of a cosmic ray telescope and electronics. Provisions for easuring the pulse height in one of the counters (not discussed in the text) are also own.

at the total flux crossing unit horizontal area is

$$2.4 \times 10^2/\text{m}^2\text{-s}. \tag{9.22b}$$

he mean energy of the muons is 2 GeV and falls off on the high side E^{-2}.

Cosmic ray muons can be easily detected by measuring the coincidence te between two scintillation counters placed vertically one above the her as shown in Fig. 9.20. By increasing the distance between the coun-rs one can restrict the solid angle acceptance and also study the angular stribution of the flux. Plastic scintillation counters have the advantage large area so that the counting rate can be several per second. If a third unter is placed in coincidence with the two-counter telescope, but is cated physically in a different location (as in Fig. 9.21) one still observes incidences.[20] These occur because *several* cosmic rays arrive at the same ne over the area covered by the telescope and the third "roving" counter.

[20]These are true coincidences after any accidental effects (Section 9.5.1) have been ntracted.

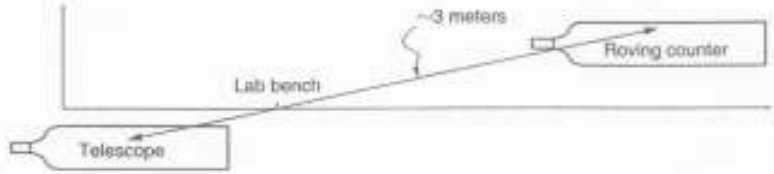

FIGURE 9.21 Arrangement of counters for measuring cosmic ray air showers (top view).

Namely a "shower" of cosmic rays occurred. One finds that the rate for such showers is 1/300 of the telescope rate, given a typical counter area of 0.2 m^2 and a displacement of 3 m.

We will describe an experiment in which cosmic ray muons are also detected by simply using a 5-gal tank of liquid scintillator, viewed by a 2-in. photomultiplier tube. Muons traversing the tank give a large signal so that it is possible to use the singles rate, without the need to form coincidences. However, the PMT high voltage and the discriminator must be set carefully. The dimensions of the tank are $d = 28$ cm diameter and $h = 35$ cm height from which we can estimate an *effective* horizontal area of $2 \times [\pi(d/2)^2] \sim 0.12\ \text{m}^2$. The singles rate is of order 25/s, in reasonable agreement with Eq. (9.22b).

9.4.2. Time of Arrival of Random Events

The arrival of cosmic rays is a random process,[21] so we expect it to follow the distributions discussed in Chapter 10. In particular when the expected number of events in a given time interval is small, the observed number should obey the Poisson distribution. Let r be the average event rate, namely the average number of events per unit time. Then the probability of observing n events in the time interval t is

$$P(n,t) = \frac{(rt)^n e^{-rt}}{n!}. \tag{9.23}$$

From Eq. (9.23) we recover the differential probability for an event ($n = 1$) to occur in the differential interval dt. Since ($dt \to 0$), Eq. (9.23) reads

$$dP = P(1, dt) = r\, dt. \tag{9.24a}$$

[21]This is of course also true for the decay of radioactive nuclei.

Similarly the probability that no events ($n = 0$) occur in the interval t is

$$P(0, t) = e^{-rt}. \tag{9.24b}$$

We can test this proposition by measuring the distribution of the time *between* the arrival of adjacent events. A time interval t between events is defined in this case by requiring *no event* for the interval t and an event at the time t (in the differential dt). Thus the distribution is given by the product of Eqs. (9.24a), (9.24b), which we write in the form[22]

$$q_1(t) = \left.\frac{dP}{dt}\right|_{m=1} = re^{-rt}. \tag{9.25}$$

It is interesting that the above distribution is exponential; namely, short time intervals t between adjacent events are much more probable[23] than longer ones.

The result for the case $m = 1$ can be generalized for the time interval between every second event ($m = 2$), every mth event, etc. The derivation is given in Section 10.5.3 (see Eq. (10.75)), and we obtain

$$q_m(t) = r\,\frac{(rt)^{m-1}e^{-rt}}{(m-1)!}, \tag{9.26}$$

As m increases, the distribution tends to a gaussian centered at $t = mr$. Of course one could also test Eq. (9.23) directly by measuring how often one, two, etc., events are found within a fixed interval t. However, measuring the distribution of the time intervals between event arrivals, as done here, is by far more practical and efficient.

Data are acquired by recording the time of arrival of every muon in a computer file. Since the mean time between counts is ~40 ms, a precision of 0.1 ms is sufficient and can be easily provided by the computer clock. The file can then be analyzed by sorting the time intervals between adjacent pulses ($m = 1$) in time bins of 0.8 ms width. The same data are next analyzed by sorting the intervals for different values of m in correspondingly longer time bins.

Results obtained by a student for $m = 1$ are shown in Fig. 9.22, for $m = 3$ in Fig. 9.23, and for $m = 100$ in Fig. 9.24. One notes how the distribution becomes narrower as m increases. Namely the interval between every

[22] We imply that the second count arrives after the first one with a delay between t and $t + dt$.

[23] This justifies the old proverb that one calamity is always followed by a second one. See W. Bothe, *Phys. Zeit.* **37**, 520 (1936).

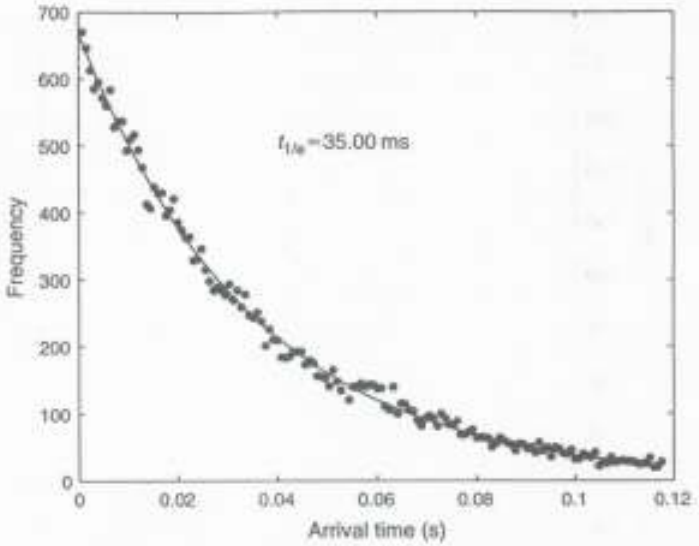

FIGURE 9.22 Distribution of the time between the arrival of two cosmic ray counts. The fit is the Poisson distribution for $m = 1$.

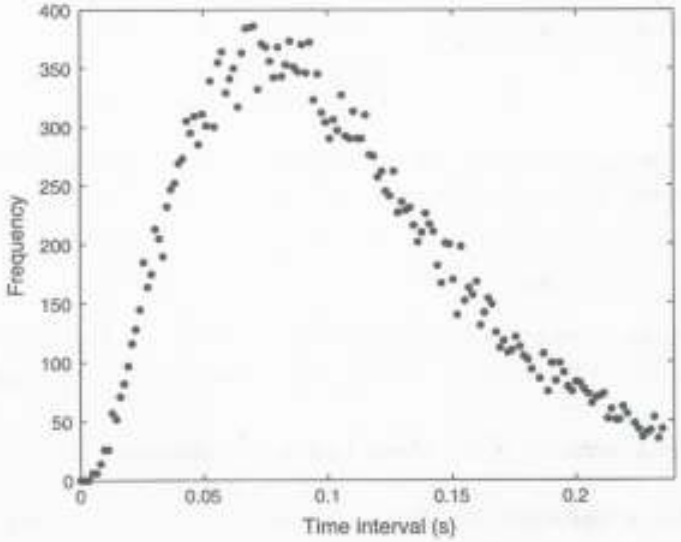

FIGURE 9.23 As described in the legend to Fig. 9.22 but for $m = 3$.

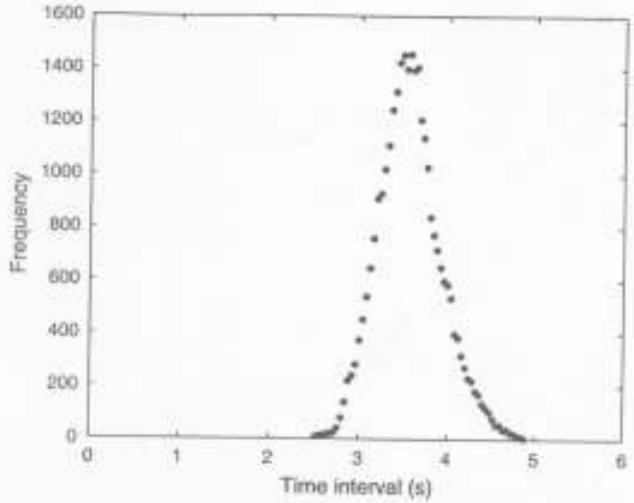

FIGURE 9.24 As described in the legend to Fig. 9.22 but for $m = 100$. Note that the distribution is centered at a mean time $t \approx 3.56$ s, where $t = (m-1)/r \approx 100/r$.

100 events is much more "stable" (relative to its mean value) than between every second event. As can be seen from Eq. (9.24) the distributions for $m > 1$ have a maximum ($dq_m/dt = 0$) at

$$t = \frac{m-1}{r}. \tag{9.27}$$

Thus, from the location of the peak in the distribution we can obtain the average rate. We find that for the data shown in Figs. 9.23, and 9.24

$$\begin{array}{lll} m = 3, & t_{\max} = 0.073 \text{ s}, & r = 27.5 \text{ /s} \\ m = 100, & = 3.56 \text{ s}, & = 27.7 \text{ /s}. \end{array}$$

Furthermore, a fit to the exponential for $m = 1$ (see Fig. 9.22) yields $t_{1/e} = 3.50 \times 10^{-2}$ s, or $r = 28.6$/s in agreement with the average rate.

9.4.3. Measurement of the Mean Life of the Muon

The muon is not stable but decays into an electron, a neutrino, and an antineutrino:

$$\begin{aligned} \mu^+ &\rightarrow e^+ + \nu_e + \overline{\nu}_\mu \\ \mu^- &\rightarrow e^- + \overline{\nu}_e + \nu_\mu. \end{aligned} \tag{9.28}$$

The mean life, or lifetime, (i.e., the inverse of the decay rate) for this process is of order 2.2 μs, and thus the decay is easily detectable for muons at rest. The neutrinos are not observable but the electron (or positron)[24] is energetic enough to give a clear signal of the decay. The mass of the muon is

$$m_\mu = 105.65 \text{ MeV/c}^2,$$

approximately 200 times the electron mass. The maximum energy of the electron occurs when the two neutrinos recoil against it as shown in Fig. 9.25a. This corresponds, in the rest frame of the muon, to

$$E_e(\max) \simeq \frac{1}{2} m_\mu c^2 = 53 \text{ MeV}.$$

The energy spectrum of the electrons from muon decay is shown in Fig. 9.25b.

The long lifetime for muon decay indicates that the decay does not proceed through the strong (nuclear) interaction but rather through the weak interaction responsible for the "β-decay" of nuclei. However, the process of Eq. (9.28) is very important because it involves only leptons (no strongly interacting particles participate) and thus can be used unambiguously to

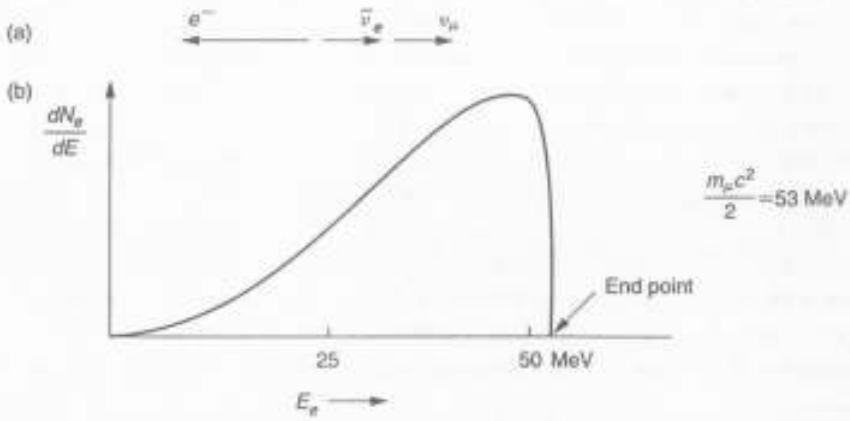

FIGURE 9.25 (a) Configuration of the particles in μ-decay for obtaining the maximum electron energy. (b) The energy spectrum of the electrons from μ-decay.

[24] To save words we will speak only of the electron even though we mean either e^- or e^+.

calculate the Fermi weak interaction constant G_F. The mean life of the muon is given by

$$\frac{1}{\tau} = \frac{1}{\hbar}\,\frac{G_F^2}{(\hbar c)^6}\,\frac{(m_\mu c^2)^5}{192\pi^3}. \tag{9.29}$$

Precise measurements of the muon mean life yield

$$\tau_\mu = (2.19703 \pm 0.00004) \times 10^{-6}\ \text{s} \tag{9.30a}$$

and through Eq. (9.29) the value of the Fermi constant[25]

$$\frac{G_F}{(\hbar c)^3} = 1.1664 \times 10^{-5}\ \text{GeV}^{-2}. \tag{9.30b}$$

We will measure the decay of muons that have come to rest in the liquid scintillator tank. Muons lose approximately 2 MeV of energy for each gram per squared centimeter of material that they traverse. Thus we expect that muons entering the 35-cm-high liquid scintillator tank with energy $E_\mu \lesssim 50$ MeV will stop in the tank. The fraction of muons that do stop is of order 0.3% of the flux going through the tank. Thus, the stopping rate is $R_S = 0.077$/s, or 4.6 muons/min. This is adequate to obtain good statistical accuracy for the mean life value in a reasonable time interval.

The experimental arrangement is shown in Fig. 9.26. When a muon enters the tank the PMT gives a signal, which is amplified and then discriminated. This pulse is used to start a "time-to-amplitude converter" (TAC) circuit. If the muon stops in the tank, then the decay electron will give a second signal within a time interval of a few mean lives. The second pulse is used to stop the TAC, and the time interval between start and stop is directly read out. The 60-ns delay in the start signal is to make sure that no pulse will be on the stop line when the start arrives. Commercial electronic modules can be used to achieve the logic indicated in Fig. 9.26. A GT200 computer card, designed by Professor D. Hartill of Cornell University,[26] performed the TAC functions and stored the data in a file in the computer memory. If no stop arrives within $\Delta t = 25$ μs, which corresponds to ~10

[25]Note that in contrast to the fine structure constant $\alpha = e^2/\hbar c$, which is dimensionless, $G_F/(\hbar c)^3$ has dimensions of inverse energy squared. In fact $G_F/(\hbar c)^3$ has the approximate value of $1/(M_W c^2)^2$, where M_W is the mass of the vector bosons that mediate the weak interactions.

[26]One can now purchase commercial versions of TAC cards to perform the required functions.

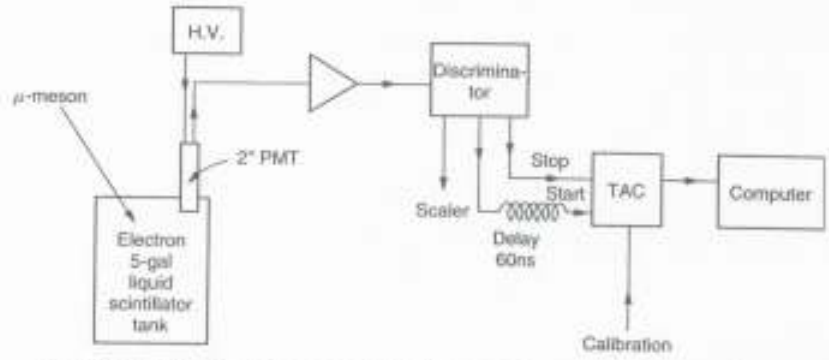

FIGURE 9.26 Block diagram of the electronics for measuring muon decay.

mean lives, the TAC is reset and the start pulse ignored. To calibrate the TAC one applies a fixed frequency (oscillator) signal to the discriminator input.

If the singles rate is too high, then the stop pulse may not be due to the decay of the muon that started the TAC, but to a different muon entering the tank. We call such events "accidental stops," and we can estimate their rates as follows. The singles rate is $r = 25$/s, so that using the Poisson distribution of Eq. (9.23) for $n = 2$ and $t = \Delta t = 25$ μs we find for the accidental rate

$$R_a = \frac{P_a(n = 2,\ \Delta t)}{\Delta t} = 7.8 \times 10^{-3}\ \text{s}^{-1}. \tag{9.31}$$

This is ten times smaller than the stopping rate R_S, and does not affect the determination of the mean life as discussed later.

Data obtained by a student are shown in Fig. 9.27. The data were accumulated over five days and yielded $N_S = 32{,}000$ stops in 6921 min. The very early events, $t < 0.25$ μs, were discarded, leaving a sample of 30,069 events displayed in 100 bins each 0.25 μs wide. The data for $t \lesssim 5$ μs show an exponential drop-off, as expected, and in this region are well fitted by

$$N(t) = N_0 e^{-t/\tau} \qquad 0.25 < t < 5\ \mu\text{s}.$$

In contrast the data for late times, $t > 15$ μs, are flat and are well fitted by a constant

$$N(t) = C \qquad 5 < t < 25\ \mu\text{s}.$$

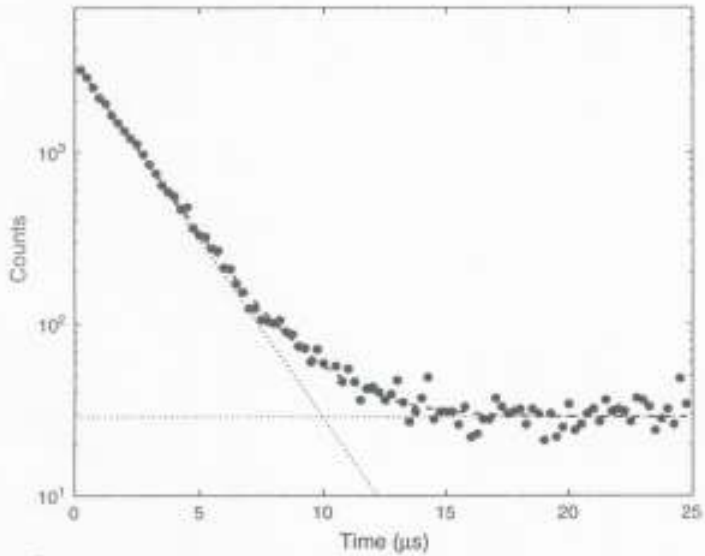

FIGURE 9.27 Data for 30,000 muon stops. The bin size is 0.25 μs, and the fit to the data including an exponential decay and a constant background term are shown.

A combined fit[27] of the form

$$N(t) = N_0 e^{-t/\tau} + C \tag{9.32}$$

yields $\tau = 2.088 \pm 0.016$ μs, $N_0 = 3410$, and $C = 28.8$, and an excellent $\chi^2 = 0.909$ per degree of freedom. The contributions of the two terms of the fit are also indicated by the dashed lines in the graph.

We briefly discuss the background level. Since there are 100 channels, the total accidental count is $N_a = 2880$, and thus the accidental rate is $R_a = N_a/6921$ min $= 6.9 \times 10^{-3}$/s in agreement with our estimate of Eq. (9.31). One recognizes that the background does not affect the measurement until

$$N_0 e^{-t/\tau} \sim C.$$

This occurs when $t/\tau \sim 4.71$, which allows for a fairly long "lever arm" to determine τ_μ.

Our value for the mean life is in close agreement with the accepted value as given in Eq. (9.30a). The agreement is even closer because the

[27] See Section 8.6.2.

measured value for τ_μ must be corrected for the following effect. When negative muons stop in matter, there is a finite probability that the μ^- will be absorbed by a proton in the nucleus, leading to a "capture" reaction:

$$\mu^- + Z \rightarrow (Z-1)^* + \nu_\mu.$$

Thus the effective mean life is shortened and given by

$$\frac{1}{\tau_e} = \frac{1}{\tau_\mu} + \frac{1}{\tau_c},$$

where $1/\tau_\mu$ and $1/\tau_c$ are the rates for decay and capture, respectively. As a result the observed mean life is shorter; for mineral oil (the capture occurs mainly on carbon nuclei) and for the μ^-/μ^+ composition of cosmic rays this correction is approximately 4%. Therefore, the corrected measured value in this experiment is

$$\tau_\mu = 2.172 \pm 0.017 \text{ μs}. \tag{9.33}$$

The error shown in Eq. (9.33) is only statistical and does not include systematic effects, in particular any uncertainty in the TAC calibration.

9.5. γ–γ ANGULAR CORRELATION MEASUREMENTS

9.5.1. General Considerations

We will now discuss the measurement of the correlation in angle between two gamma rays that were emitted simultaneously from the same source. The origin of these gamma rays is frequently the cascaded decay of a nucleus, as in the case of ^{60}Ni (^{60}Co) already discussed in Chapter 8. (See Fig. 8.20.) We reproduce in Fig. 9.28 the decay scheme of this nucleus and note that the 1.333-MeV gamma ray follows the 1.172-MeV gamma ray, the lifetime of the intermediate state being only about 10^{-12} s, so that for all practical purposes the two gamma rays are coincident.

The fact that these two gamma rays are correlated in angle can be understood from the following general argument: the first gamma ray will have an angular distribution with respect to the spin axis of the nucleus; thus its observation at a fixed angle $\theta = 0$ conveys information about the probability of finding the spin at some angle ψ with respect to the